

## Support Information

### **Antimicrobial peptides modification enhances the gene delivery and bactericidal efficiency of gold nanoparticles for accelerating diabetic wound healing**

Song Wang<sup>a</sup>, Chang Yan<sup>b</sup>, Ximu Zhang<sup>c</sup>, Dezhi Shi<sup>d</sup>, Luxiang Chi<sup>b\*</sup>, Gaoxing Luo<sup>a\*</sup>, Jun Deng<sup>a\*</sup>

- a. Institute of Burn Research, Southwest Hospital, State Key Lab of Trauma, Burn and Combined Injury, Third Military Medical University (Army Medical University), Chongqing 400038, China.
- b. Department of Cardiology, Southwest Hospital, Third Military Medical University (Army Medical University), Chongqing 400038, China.
- c. Chongqing Key Laboratory of Oral Disease and Biomedical Sciences & Chongqing Municipal Key Laboratory of Oral Biomedical Engineering of Higher Education & Stomatological Hospital of Chongqing Medical University, Chongqing 401174, China.
- d. Key Laboratory of Three Gorges Reservoir Region's Eco-Environment, Ministry of Education, Faculty of Urban Construction and Environmental Engineering, Chongqing University, Chongqing 40005, PR China

\* Corresponding authors.

E-mail addresses: [chi68754271@126.com](mailto:chi68754271@126.com) (L. Chi), [logxw@yahoo.com](mailto:logxw@yahoo.com) (G. Luo),  
[djun.123@163.com](mailto:djun.123@163.com) (J. Deng)

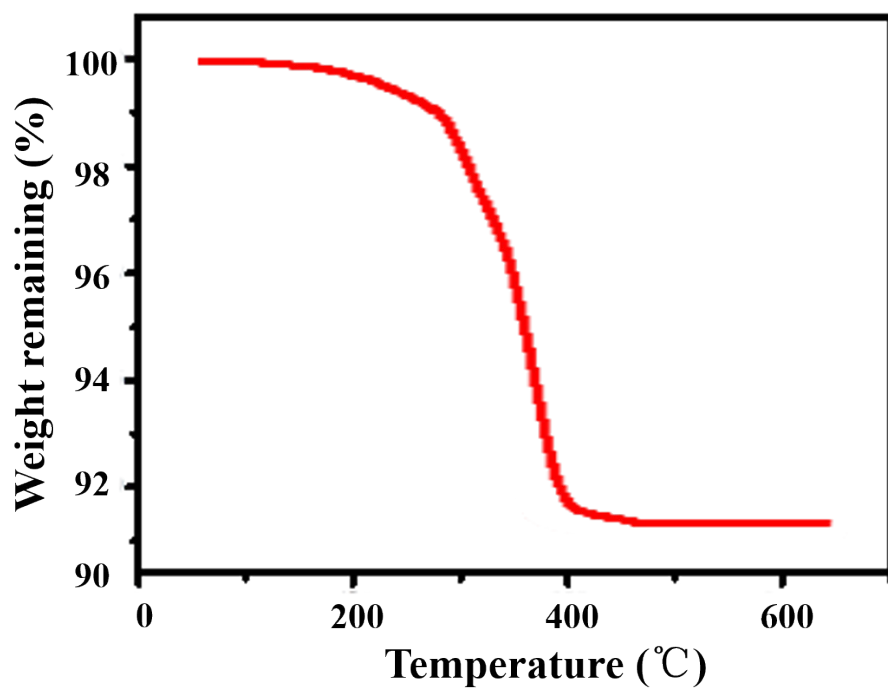


**Figure S1** Thermogravimetric analysis of the PEI protected AuNPs.

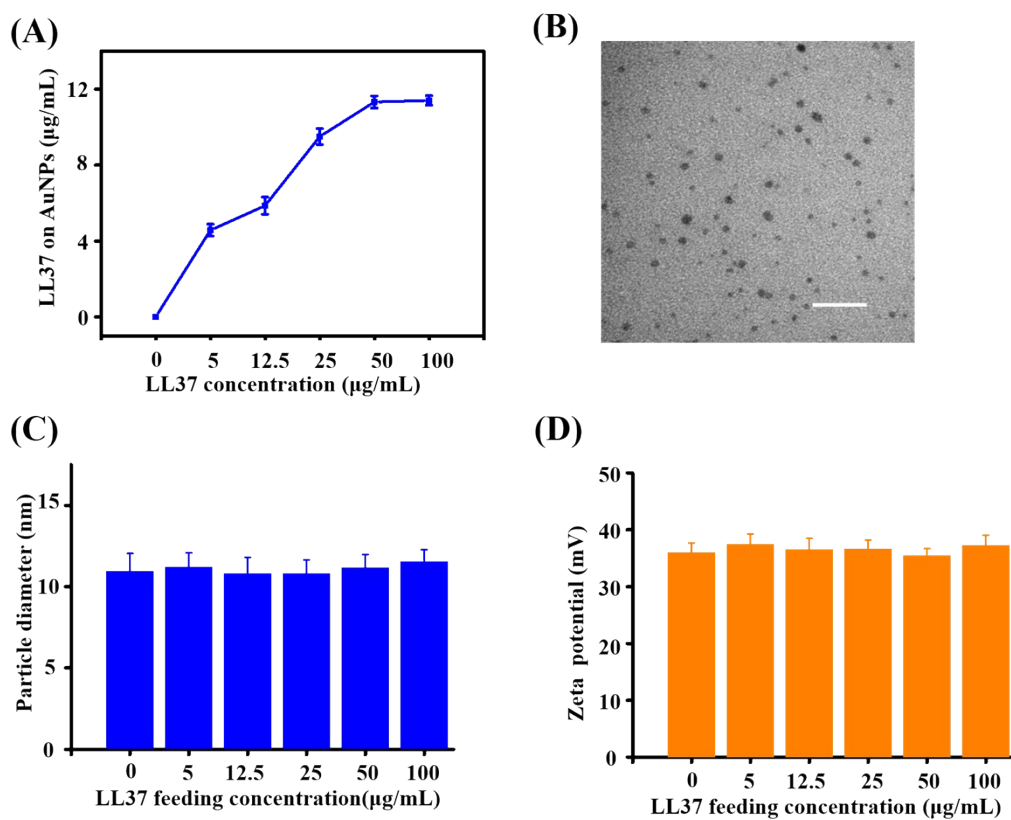


**Figure S2** (A) The analysis of peptide content on AuNPs (n=5). (B) TEM images of AuNPs@LL37. (C) Particle and (D) Zeta potential of AuNPs@LL37 (n=5).

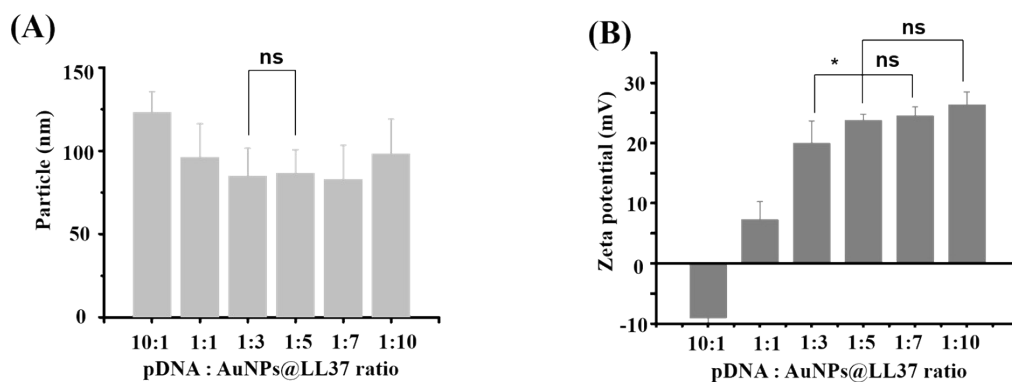


**Figure S3** Effect of pDNA:AuNPs@LL37 ratio on (A) the hydrodynamic diameter and (B) zeta potential of the AuNPs@LL37 /pDNA complex (n=5), (\* presents  $p < 0.05$ , NS=no significance).

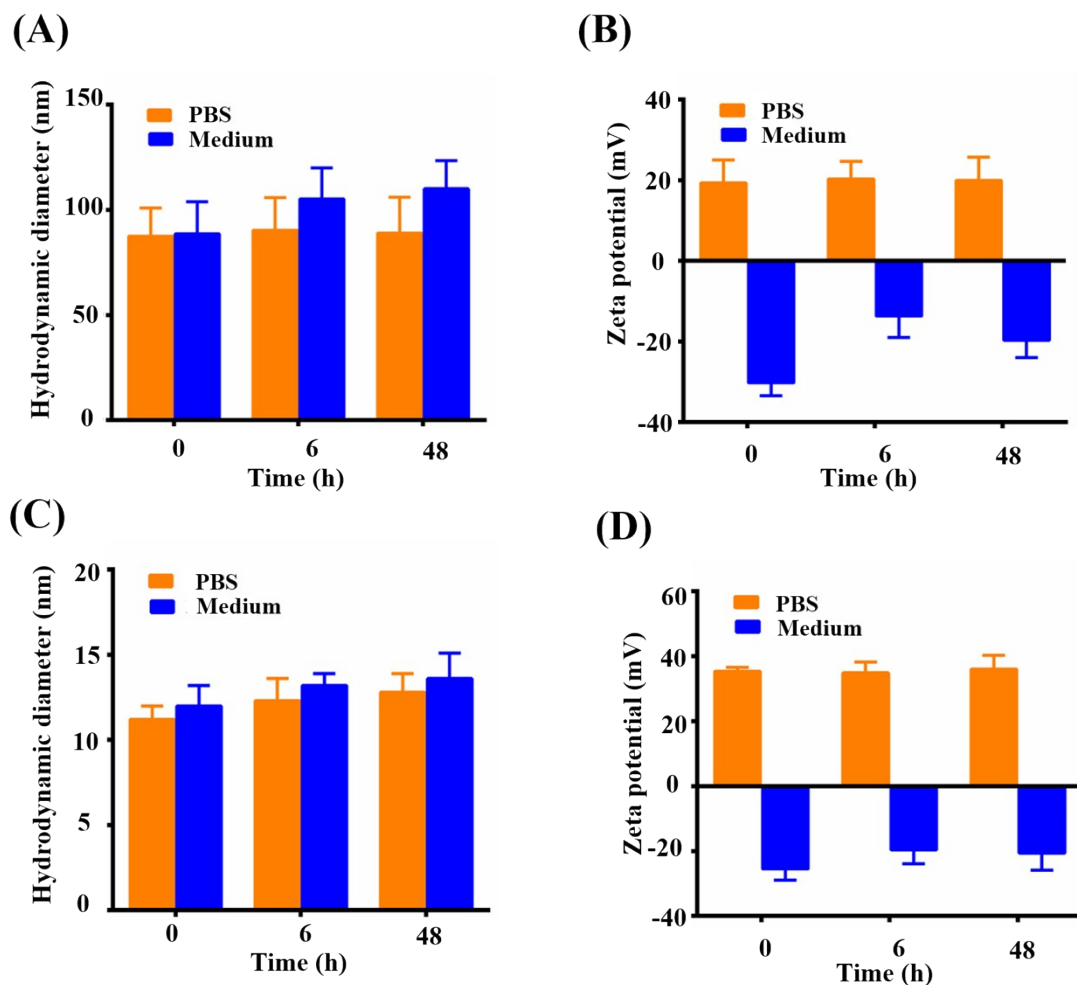


**Figure S4** Stability assessment of AuNPs@LL37/pDNAs and AuNPs/pDNAs suspended in complete keratinocyte culture medium. Hydrodynamic diameter of (A) AuNPs@LL37/pDNAs and (C) AuNPs/pDNAs (n=5). The zeta potential of (B) AuNPs@LL37/pDNAs and (D) AuNPs/pDNAs (n=5). The NPs were suspended in PBS or complete keratinocyte medium.

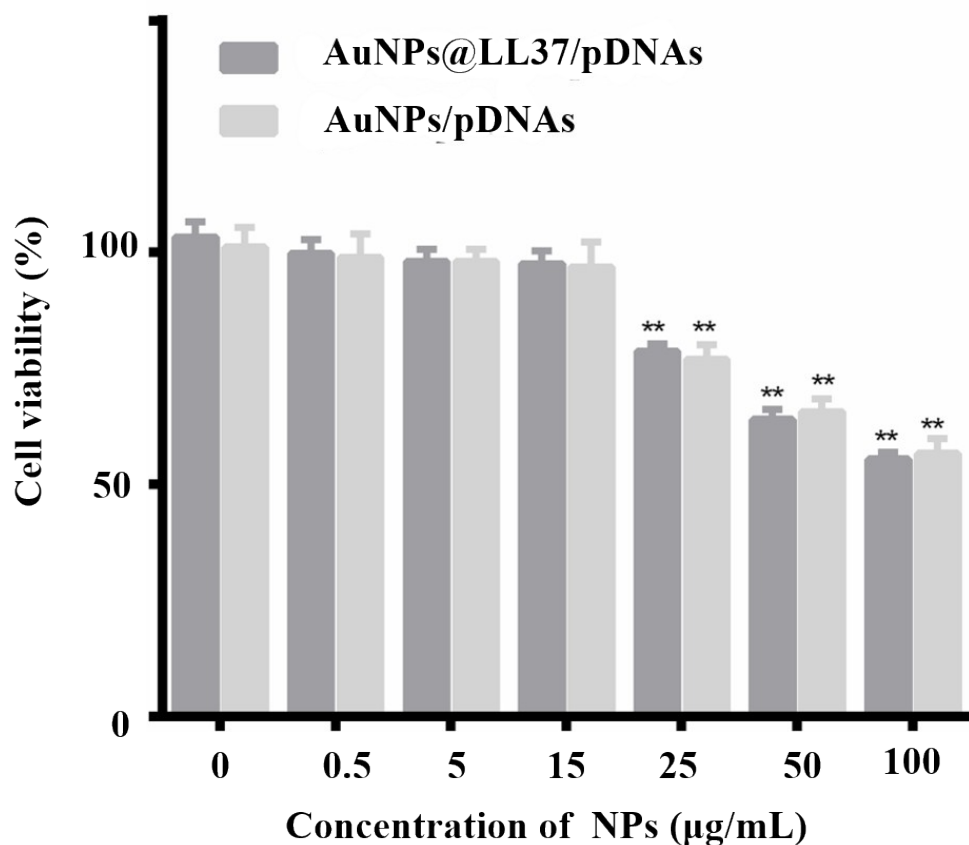


**Figure S5** *In vitro* cytotoxicity of AuNPs@LL37/pDNAs. Keratinocytes were treated with different concentrations of AuNPs@LL37/pDNAs for 48 h (n=5). \* and \*\* present significant difference (Compared with control groups) at  $p < 0.05$  and  $p < 0.01$  levels, separately.

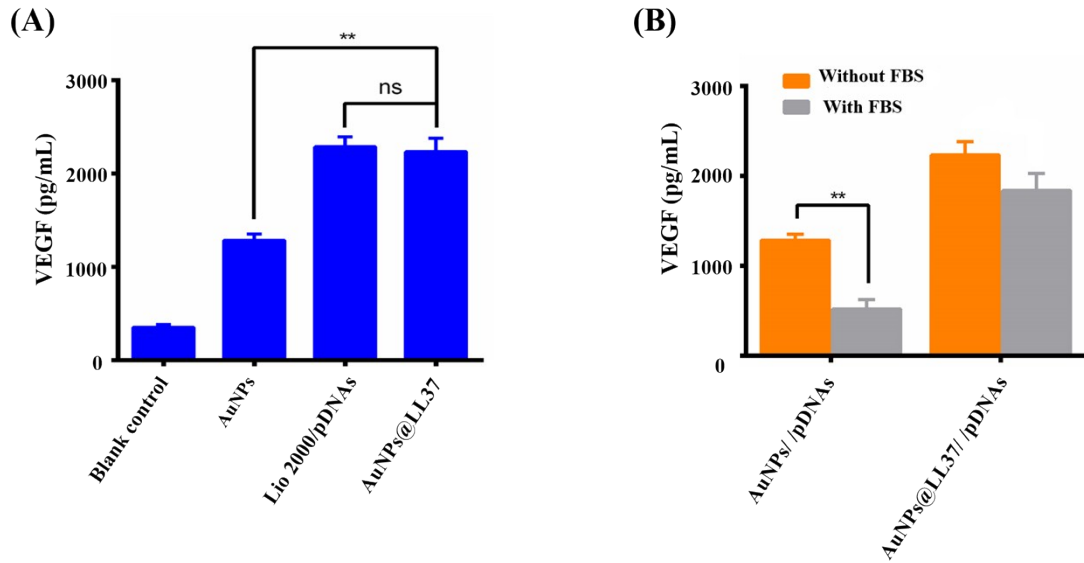


**Figure S6** VEGF expression levels from transfected keratinocytes. (A) VEGF levels from keratinocytes with various treatments. (B): VEGF expression levels from keratinocytes with AuNPs/pDNAs and AuNPs@LL37/pDNAs treatments in the presence or absence of 10% FBS (n=5), respectively. \*  $p < 0.05$ , NS=non-significance.

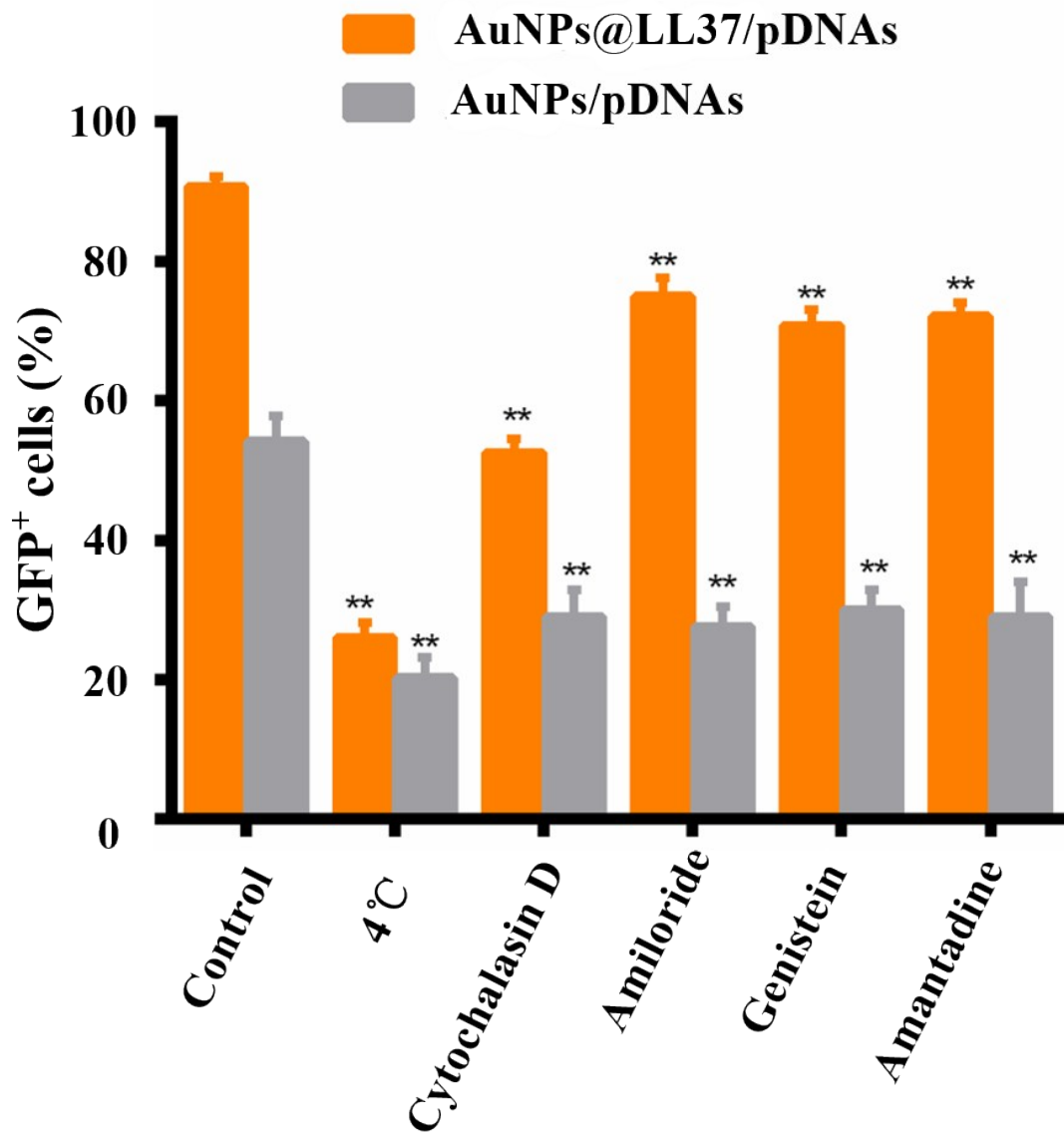


**Figure S7** Flow cytometry analysis of GFP<sup>+</sup> cells fraction in keratinocytes with AuNPs@LL37/pDNAs treated (n=3). Cells were pretreated by amantadine-HCl, genistein, amiloride-HCl, cytochalasin D, or under 4 °C for 30 min, respectively. \*\* indicates a significant difference at p<0.01 level vs individual inhibitor-free control.

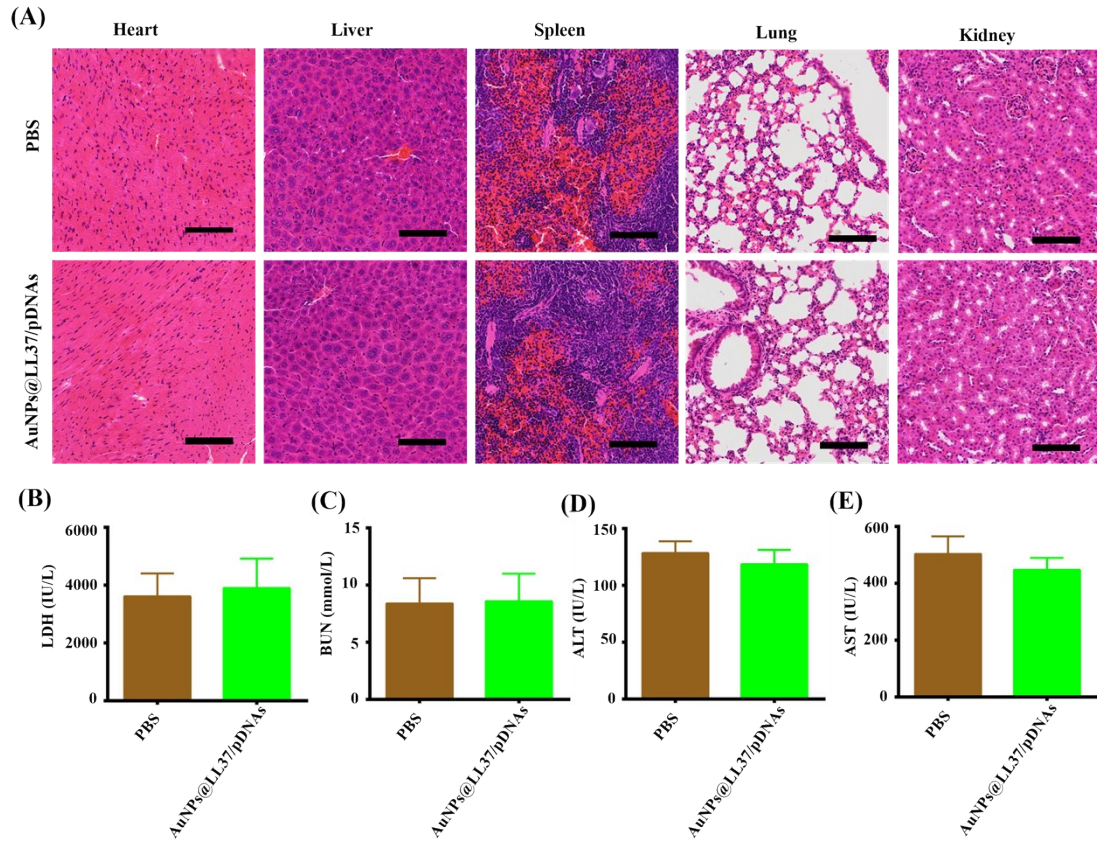


**Figure S8** Biocompatibility evaluation of AuNPs@LL37/pDNAs *in vivo*. (A) H&E staining images of the major organs from PBS control mice and AuNPs@LL37/pDNAs at a concentration of 837.7  $\mu\text{g}/\text{mL}$  (30 days after injection). (B) *In vivo* assessment of biochemical parameters from mice treated with PBS and AuNPs@LL37/pDNAs on the 30th day after injury (n=5). \*\* indicates a significant difference at  $p < 0.01$  level vs PBS treated control.